Numerical Simulation of the Spatial Turbulent Mixing Supersonic Forced Jets in CoFlow

AKERKEH ZADAULY[1], ASEL BEKETAEVA[2], ALTYNSHASH NAIMANOVA[3]
1. Institute of Mechanics and Engineering Science, Almaty, Kazakhstan
(e-mail: azadauly@gmail.com)
2. Al-Farabi Kazakh National University, Almaty, Kazakhstan (corresponding author to provide phone: +7(727)272-00-48; e-mail: azimaras10@gmail.com).
3. Institute of Mathematics and Mathematical Modeling, Almaty, Kazakhstan
(e-mail: alt_naimanova@yahoo.com).

Abstract:— The most significant problem in many industrial applications such as flows in combustors and nozzles is the study of mixing properties of jets. At present, the problem of control of enhancing the mixing in the low-speed flows is well studied while in the high-speed flows this problem is still important. In this paper the supersonic turbulent forced jet of perfect gas in a supersonic coflow is studied numerically. The simulation is performed using the three-dimensional LES filtered Navier–Stokes equations coupled with the Smagorinsky turbulence model, the solution of which is based on the third-order non-oscillatory (ENO) scheme. For the turbulent jet control and the mixing enhancement problems the inlet deterministic excitation (forcing) with various frequencies and perturbation amplitudes is proposed. It is revealed that the behaviour of the growth of shear layer is governed with deterministic forcing at the entrance. A namely, including forcing gives much more quickly pairing of the vortices and the rise of thickness of shear layer in compare to the 'natural' jet (without forcing). Additionally, the variation of excitation frequency nonuniformly influences on the rolling up of the vortices; the decrease of frequencies slows down roll-up process and enlarges vortices stretch in the streamwise direction. The obtained turbulence properties are in good agreement with experimental data.

Keywords:— Numerical simulation, supersonic jet, perfect gas, Navier-Stokes equations, mixing enhancement, forced jet, spectral initial conditions.

1 Introduction

The study of the mixing properties of jets has an important role in many industrial applications such as: turbulent mixing of the jet of fuel with flowing air in the combustion chambers, jet interactions at the launch of rocket and space mechanism with launch equipment etc. The problem of enhancing the mixing has been explored by many authors both experimentally [1]-[8], [18] and numerically [9]-[17].

For example, the comparison of the two jet regimes:
1) the natural jet (which mimicked a realistic experimental profile of coaxial jets), 2) the natural jet with additional excitations; has been performed numerically with the DNS approach [13]. They revealed that imposing of the additional forcing to the jet gave more homogenous mixing without a spot of unmixed fluid.

In the [14] jet shear layers were excited over a series of excitation Strouhal numbers and azimuthal modes (axisymmetric, helical, and flapping).

The wide variation in the preferred mode of Strouhal number was shown to be tightly linked to evolution, spacing, and scale of the coherent flow structures, which dominated the jet shear layer's development.

The study of the vortex dynamics and the statistics of bifurcating jets was performed in [15]. Authors analyzed in detail the three-dimensional coherent structures resulted from every case of specific forcing and explained their impact on the statistical behavior of bifurcating jets. They found out the most efficient strategy of jet control was a combination of an axisymmetric excitation of the preferred frequency and a flapping excitation at the subharmonic frequency.

The detailed survey of the shear flow research on active and passive control of flows relevant to propulsion applications, with an emphasis on exploring the underlying low mechanisms was given in [16]. A namely, the advantages and the disadvantages of the following excitation: artificial excitation of jets, natural excitation and screech,

complex nozzles, induced screech and multi-jets, studies of excitation techniques and other aspects of jet flows, passive control by tabs, flow separation control and dynamic stall were discussed.

In [17] the mixing efficiency improvement problem was studied on example of the gaseous jets with and without additional excitation using the LES approach. Authors revealed that the application of the low energetic small amplitude excitation of the gas phase resulted in bifurcating jet.

The experimental result of the study of steady and pulsed control jets in enhancing the mixing rate of a high Reynolds number and high subsonic Mach number jet has been represented in [18]. This study has shown that the use of control jets (steady and pulsed) was an effective mixing enhancement technique. The results revealed that significant potential core length reduction has been achieved by using the control jets. The jet cross section became highly asymmetric and the jet-spreading rate increased considerably in the orthogonal plane in the case of the control jets.

Most of the above mentioned studies analyzed low-speed flows though the problem of control of enhancing the mixing in high-speed jets is still open. The aim of this paper is the numerical study of supersonic turbulent forced jet of perfect gas in coflow with a focus on the mixing control. The schematic diagram of the flow is shown in Fig.1.1:

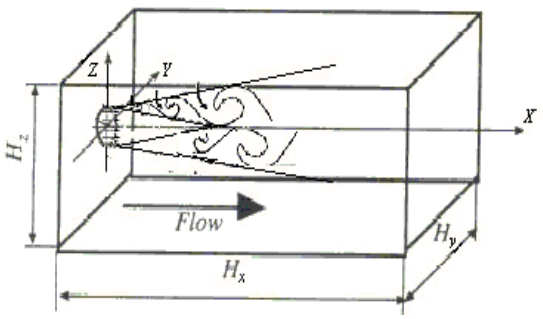

Fig.1.1. Schematic diagram of the computational domain

2 Physical models and numerical methods

2.1 Governing Equations

Basic equations for the problem are the system of the three-dimensional filtered by the LES Navier-Stokes equations for the compressible turbulent perfect gas in the Cartesian coordinate system written in the conservative form as:

$$\frac{\partial \vec{U}}{\partial t}+\frac{\partial\left(\vec{E}-\vec{E}_v\right)}{\partial x}+\frac{\partial\left(\vec{F}-\vec{F}_v\right)}{\partial y}+\frac{\partial\left(\vec{G}-\vec{G}_v\right)}{\partial z}=0, \qquad (1)$$

where vectors of dependent variables and vector fluxes are defined by

$$\vec{U}=\left(\rho,\rho u,\rho v,\rho w,E_t\right)^T,$$
$$\vec{E}=\left(\rho u,\rho u^2+P,\rho uv,\rho uw,\left(E_t+P\right)u\right)^T,$$
$$\vec{F}=\left(\rho v,\rho uv,\rho v^2+P,\rho vw,\left(E_t+P\right)v\right)^T,$$
$$\vec{G}=\left(\rho w,\rho uw,\rho vw,\rho w^2+P,\left(E_t+P\right)w\right)^T,$$
$$\vec{E}_v=\left(0,\tau_{xx},\tau_{xy},\tau_{xz},u\tau_{xx}+v\tau_{xy}+w\tau_{xz}-q_x\right)^T$$
$$\vec{F}_v=\left(0,\tau_{xy},\tau_{yy},\tau_{yz},u\tau_{xy}+v\tau_{yy}+w\tau_{yz}-q_y\right)^T$$
$$\vec{G}_v=\left(0,\tau_{xz},\tau_{yz},\tau_{zz},u\tau_{xz}+v\tau_{yz}+w\tau_{zz}-q_z\right)^T$$

Components of the viscous stress tensor are given as:

$$\tau_{xx}=\frac{2\mu_{eff}}{3\mathrm{Re}}\left(2u_x-v_y-w_z\right)$$
$$\tau_{yy}=\frac{2\mu_{eff}}{3\mathrm{Re}}\left(2v_y-u_x-w_z\right),$$
$$\tau_{zz}=\frac{2\mu_{eff}}{3\mathrm{Re}}\left(2w_z-u_x-v_y\right),$$
$$\tau_{xy}=\tau_{yx}=\frac{\mu_{eff}}{\mathrm{Re}}\left(u_y+v_x\right),$$
$$\tau_{xz}=\tau_{zx}=\frac{\mu_{eff}}{\mathrm{Re}}\left(u_z+w_x\right),$$
$$\tau_{yz}=\tau_{zy}=\frac{\mu_{eff}}{\mathrm{Re}}\left(v_z+w_y\right).$$

The heat flux is defined by

$$q_x=-\frac{\mu_{eff}}{(\gamma-1)M_\infty^2\mathrm{PrRe}}T_x$$
$$q_y=-\frac{\mu_{eff}}{(\gamma-1)M_\infty^2\mathrm{PrRe}}T_y$$
$$q_z=-\frac{\mu_{eff}}{(\gamma-1)M_\infty^2\mathrm{PrRe}}T_z.$$

The effective viscosity is equal to the sum of two

viscosities: $\mu_{eff} = \mu_l + \mu_{sgs}$, where μ_l is determined by the Sutherland formula and μ_{sgs}:

$$\mu_{sgs} = \rho(C\Delta)^2\sqrt{\tilde{S}_{ij}\tilde{S}_{ij}}, \quad (2)$$
$$\tilde{S}_{ij} = \frac{1}{2}\left(\frac{\partial\tilde{u}_i}{\partial x_j} + \frac{\partial\tilde{u}_j}{\partial x_i}\right), i = 1,2,3,\ j = 1,2,3$$

where C is the model coefficient which is varied during the simulations, Δ is the width of filter which is equal to the spatial step.

The pressure and the temperature are given as:

$$P = (\gamma - 1)\left[E_t - \frac{1}{2}\left(\rho u^2 + \rho w^2 + \rho v^2\right)\right], \quad (3)$$
$$T = \left(\frac{1}{\rho c_v}\right)\left[E_t - \frac{1}{2}\left(\rho u^2 + \rho w^2 + \rho v^2\right)\right],$$
$$c_v = \frac{1}{\gamma(\gamma - 1)M_\infty^2}.$$

In the system (1) u, w, v represent the components of the velocity vector, ρ is the density, c_v is the specific heat at constant volume, γ is the ratio of specific heats, M_∞ is the flow Mach number.

The system of equations (1) is converted to the non-dimensional form, where the flow parameters $u_\infty, \rho_\infty, T_\infty$ are taken as reference values, for the pressure P and the total energy E_t the reference values are $\rho_\infty u_\infty^2$, the length scale is the initial vorticity thickness of a mixing layer :

$$\delta_\theta(x) = \int_{-H/2}^{+H/2} (\overline{\rho}(\tilde{u} - u_\infty)\cdot(u_0 - \tilde{u})/(\rho_\infty \Delta u^2))dz$$

where $\tilde{u} = (u - u_\infty)/\Delta u \quad \Delta u = u_0 - u_\infty$

Pr, Re are the Prandtl and Reynolds numbers. Index 0 corresponds to the parameters of the jet and index ∞ corresponds to the parameters of the flow.

2.2 Boundary and initial conditions

At the channel entrance the inlet condition is given by a velocity profile in the way:

$$\vec{V}(x_i,t) = \vec{V}(x_i)^{base} + \vec{V}(x_i,t)^{natural} + \vec{V}(x_i,t)^{forced} \quad (4)$$

where $\vec{V} = (u, v, w),\ (x_i) = (x, y, z)$

$\vec{V}(x_i)^{base}$ is the velocity field given as follows:

$$\vec{V}(x_i)^{base} = \begin{cases} u_\infty = 1, v_\infty = 0, w_\infty = 0, \\ for \quad x = 0, 0 \le y \le H_y, 0 \le z \le H_z \\ u_0 = \sqrt{T_0}\,\dfrac{M_0}{M_\infty}, v_0 = 0, w_0 = 0, \\ for \quad x = 0, \quad \left|z^2 + y^2\right| \le R \end{cases}$$

and in the shear layer of the thickness δ_θ the hyperbolic tangent function is taken:

$$\phi(z) = 0.5(\phi_0 + \phi_\infty) + 0.5(\phi_0 - \phi_\infty)\tanh(0.5z/\delta_\theta) \quad (5)$$

where $\phi = (u, v, w)$.

Here H_x, H_y and H_z are length, width, and height of the computational domain, respectively, and R is the radius of the jet orifice.

Methods, using preliminary calculation (recycling methods), generate values in the additional zone, and then these values are used as boundary condition at the entrance in the main zone [19]-[21]. It was obtained that these methods can only be used in the homogeneous flows, for example, the completely turbulent flows. In the algebraic and spectral methods a set of random numbers, satisfying the given statistic values of the turbulence is used [22]-[24].

The ways of imposing the anisotropy and the inhomogeneity into the velocity field in the spectral methods leads to the similarity between the simulated turbulence and the real turbulence. From review of literature it follows that the more perspective are the spectral methods, since these methods provide the most real view of investigated flow. Key part of the method is the imposing of an anisotropic field of perturbations including the set of random numbers, satisfying the given statistic values of the turbulence.

In agree with the above the "natural" fluctuation velocity field at the entrance $\vec{V}(x_i,t)^{natural}$ from (4) is given by analogy as in [23], and the spectral boundary conditions at the entrance for this case are as follows:

$$\vec{V}'(x_i,t) = 0.5 \cdot \sum_{n=1}^{N} \sqrt{q^n}\left[\cos(k^n \cdot d \cdot x_i + \varphi_n)\right] \quad (6)$$

where d is the random frequency and φ_n is the random phase shift, both determined in the interval [0;1], here N taken as $N=100$ and q^n is the normalized amplitude :

$$q^n = \frac{E(k^n)\Delta k^n}{\sum_{n=1}^{N} E(k^n)\Delta k^n}, \qquad \sum_{n=1}^{N} q^n = 1$$

where *E(k)* is the modified von Karman energy spectrum:

$$E(k) = \frac{(k/k_e)^4}{[1+2.4(k/k_e)^2]^{17/6}} \quad (7)$$

where

$$k^n = k^{\min} \cdot (1+\alpha)^{n-1}, \quad n = 1 \div N, \quad \alpha = 0.01$$
$$k^{\min} = \beta \cdot k_e^{\min}, \beta \le 1, k_e^{\min} = 2\pi / l_e^{\max},$$
$$l_e^{\max} = \max(h_x, h_z, h_y)$$

The forced velocity $\vec{V}(x_i,t)^{forced}$ is given in the following form:

$$\vec{V}'(x_i,t)^{forced} = A \cdot G(z) \cdot \sin(\omega \cdot t) + B \cdot G(z) \cdot \cos(\omega \cdot t) + C \cdot G(z) \cdot \sin(\omega \cdot t) \cdot \cos(\omega \cdot t) \quad (8)$$

In (8) $G(z)$ is the Gauss function $G(z) = \exp(-z^2/2\delta_\theta^2)$, A, B and C are the perturbation amplitudes taken in the range of 3-10% of the velocity $\vec{V}(x_i)^{base}$, ω is the excitation frequency, which is determined either from experiments or estimated using the linear stability theory [25]-[26].

In the output and the lateral boundaries the non reflective boundary conditions are specified [27].

2.3 Numerical Schemes

Preliminary, at the level of the jet injection, a thickening of the grid is introduced for a more accurate numerical solution. Then the system (1) in the transformed coordinate system is written in the form:

$$\frac{\partial \tilde{U}}{\partial t} + \frac{\partial \tilde{E}}{\partial \xi} + \frac{\partial \tilde{F}}{\partial \zeta} + \frac{\partial \tilde{G}}{\partial \eta} = \frac{\partial \tilde{E}_v}{\partial \xi} + \frac{\partial \tilde{F}_v}{\partial \zeta} + \frac{\partial \tilde{G}_v}{\partial \eta} \quad (9)$$

where $\tilde{U} = \vec{U}/J$, $\tilde{E} = \xi_x \vec{E}/J$, $\tilde{F} = \zeta_y \vec{F}/J$, $\tilde{G} = \eta_z \vec{G}/J$, $\tilde{E}_v = \xi_x \vec{E}_v/J$, $\tilde{F}_v = \zeta_y \vec{F}_v/J$, $\tilde{G} = \eta_z \vec{G}_v/J$ and $J = \partial(\xi,\zeta,\eta)/\partial(x,y,z)$ is the Jacobian transform.

The solution of the system (9) is performed with semi-implicit method proposed in [28,29].

Firstly, the linearization procedure is applied to the equations (9). Then, the factored scheme of the linearized system is written. This form reduced the three-dimensional matrix inversion problem to the three one-dimensional problems in directions ξ, ζ and η. Secondly, the obtained one-dimensional problems are solved implicitly with matrix sweep method for the vector $\tilde{U}$. Here, the advective terms are approximated using the third-order ENO scheme in detail represented by authors in [28, 29]. The central differences of the second order accuracy are used for approximation of diffusion terms.

3 Results and discussion

The verification of the numerical model is conducted by the comparison of the computational results with the experimental data of [30] for the problem of the shear layer, where two parallel flows with different Mach numbers are given with following parameters:

M_1	M_2	M_c	U_1/U_2	ρ_1/ρ_2
1.80	0.51	0.51	0.36	0.64

where $M_c = (U_1 - U_c)/a_1, (a_1U_2 + a_2U_1)/(a_1+a_2)$ is the convective Mach number and U_1, U_2 are the velocities of the upper (index 1) and the lower (index 2) flows respectively and a_1, a_2 are the local sound velocities of the flows. The pressure on the entrance is constant for two flows, the size of domain is: $H_x = 60$, $H_y = 20$, $H_z = 20$ and the computational grid is of 271x101x101 nodes.

The results of comparison of turbulent quantities with experiments are shown in Fig. 3.1-3.3 for the

cross section with x = 18. For streamwise and lateral turbulence intensities and Reynolds stress profiles the good agreement with experiment is obtained.

Below represented the results of numerical simulation of the stated problem with following parameters: $M_\infty = 1$, $M_0 = 2$, $\mathrm{Re} = 10^5$, the diameter of orifice is $d = 6$, the pressure $P = 1atm$ is constant. The size of computational domain is: $H_x = 200$, $H_y = 30$, $H_z = 30$ and the jet center is located at the point with the coordinates $y_0 = 25$, $z_0 = 25$.

Fig. 3.4 represents the dynamic of the vortices structures in the shear layer solved without forcing of the jet. The result shows that to the time t = 37.5 the vortices are started formed and they are moving downstream (Fig. 3.4 (b)). Pairing of the adjacent vortices with forming the larger ones is demonstrated in Fig.3.4 (c). And the relatively stable turbulence occurs to the time t = 62,5 (Fig.3.4 (d)).

In Fig. 3.5 – 3.6 the results with and without forcing of the jet are represented. For the excited jet in the boundary condition (8) at the entrance for streamwise velocity the parameters taken as: A = 0.06, B = 0, C = *0*, and for the transverse velocities: A = 0, B = 0.06, C = 0 with frequencies: $\omega = \pi / 6, \pi / 9, \pi / 12$.

From comparison of the figures, it is visible (Fig. 3.5) that in the "natural" case (Fig.3.5 (a)) the formation of the vorticities is occurred much later. While including the excitation for all three frequencies (Fig. 3.5 (b-d)) gives much more quickly pairing of the vortices and growth of their sizes. Additionally, Fig.3.6 shows that the variation of the frequency nonuniformly influences on the growth and pairing of the vortices.

The growth of the shear layer is shown on the picture of the vorticity thickness $\delta_\omega = \dfrac{u_\infty - u_0}{(\partial u / \partial z)_{\max}}$ in Fig 3.7 for frequencies $\omega = \pi / 6, \pi / 9, \pi / 12$. This picture demonstrates nonlinear growth of the vorticity thickness for all cases. From figure it is visible that for the excited jet with frequency $\omega = \pi / 9$, the lines are higher compared to others. Apparently, this is due to the fact that in the case of $\omega = \pi / 6$ (Fig.3.6 b) the roll-up process is quicker, in comparison with others (Fig.3.6 c, d), consequently, the density of the formed vortices is higher.

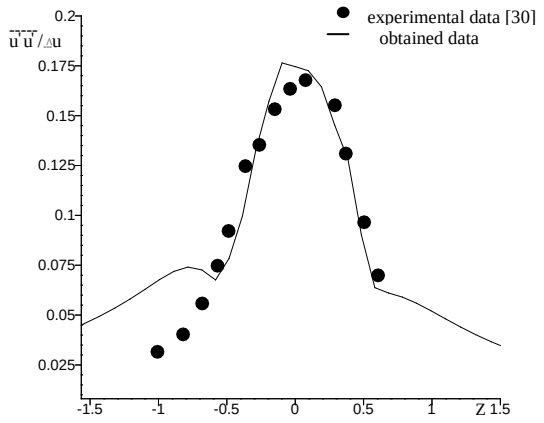

Fig. 3.1. Streamwise turbulence intensities

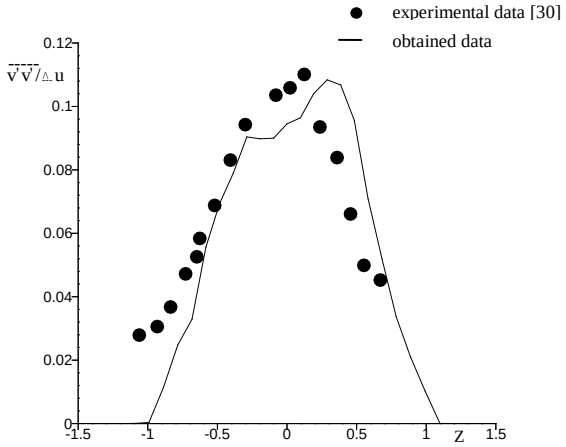

Fig. 3.2. Lateral turbulence intensities.

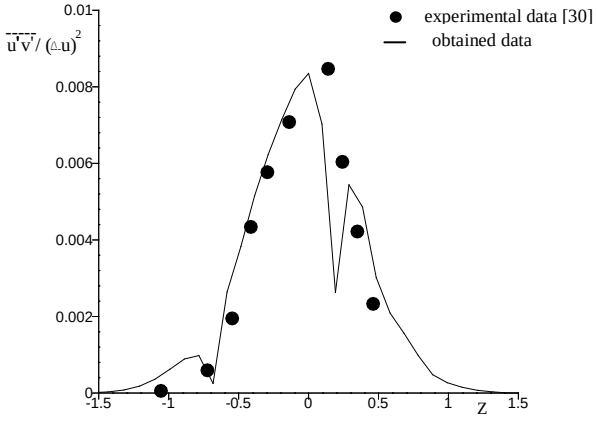

Fig. 3.3. The Reynolds stress profiles

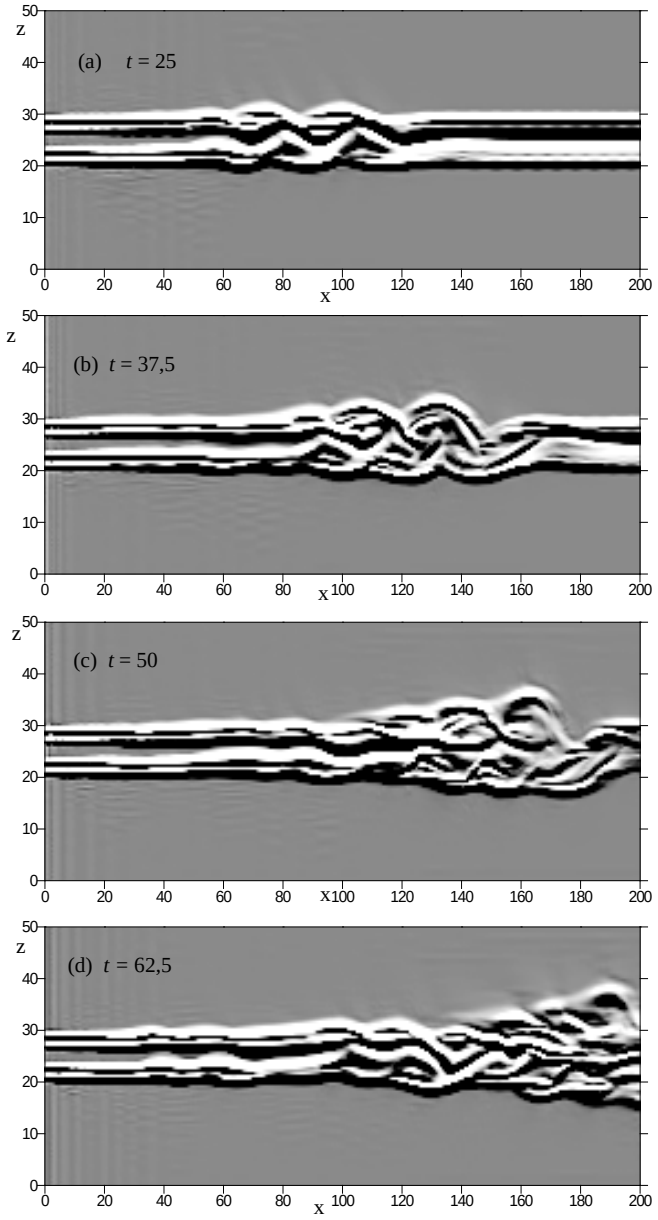

Fig. 3.4. Evolution of vorticity isolines at various times for natural jet in co-flow

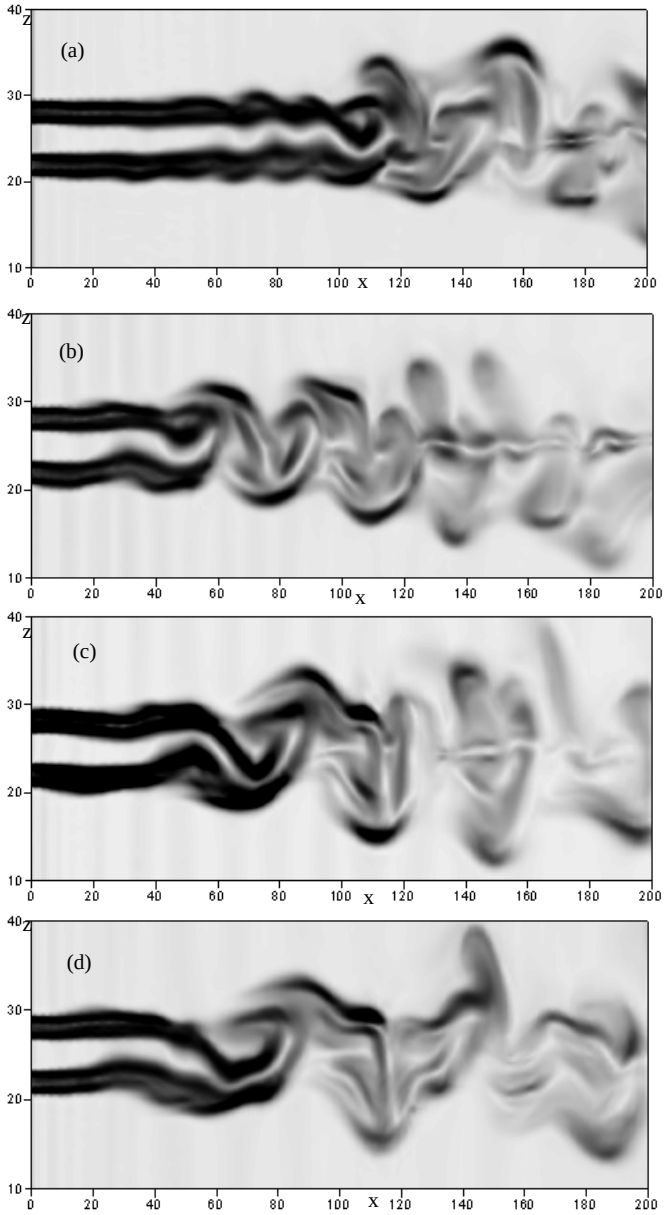

Fig. 3.5. Isolines of vorticity for natural jet in co-flow (a) and forced jet in co-flow with various frequencies: (b) $\pi/6$, (c) $\pi/9$ and (d) $\pi/12$

The decrease of the frequencies slows down the pairing process and enlarges vortices stretch in the streamwise direction which gives the growth of the vortices thickness (Fig. 3.7 c, d). However, the vorticity thickness in the case of $\omega = \pi/12$ decreases because of the too much stretching of vortices in the streamwise direction. (Fig. 3.7 d).

The isolines of vorticities (Fig. 3.8) and the distribution of vorticity thickness (Fig. 3.9) are illustrated the influence of the excited jet with $\omega = \pi/9$ to the mixing properties.

The result shows that the increase of amplitudes from 0.03 to 0.1 gives growth of the maximum of δ_ω from 30 to the 135 (Fig. 3.9).

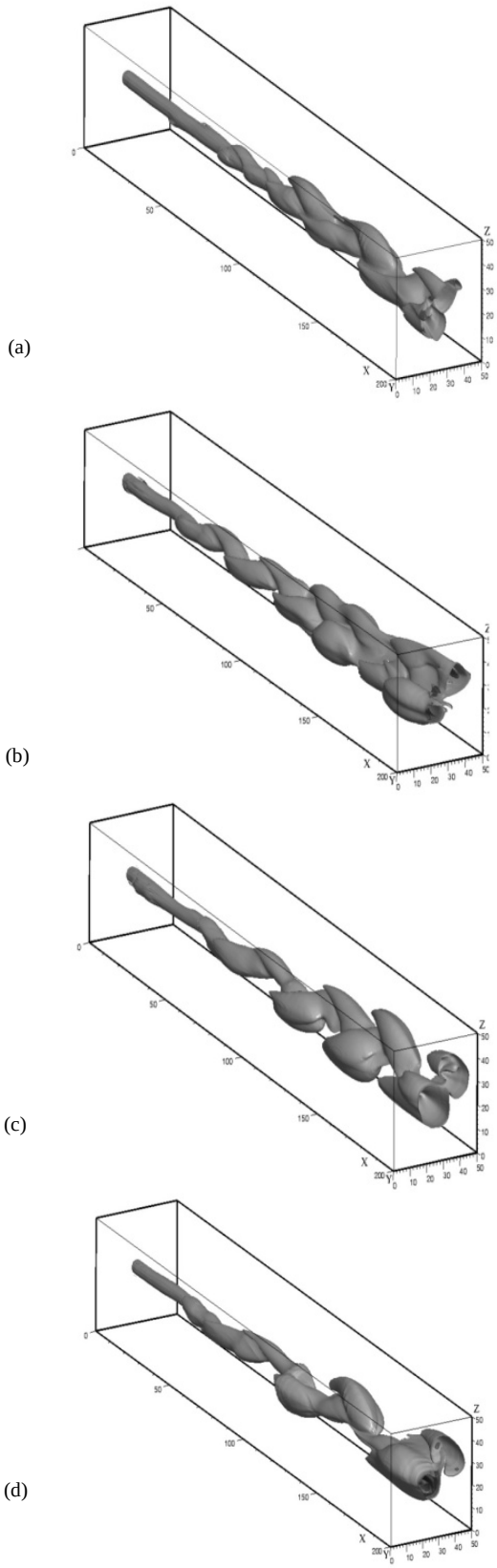

Fig. 3.6. Instantaneous isosurface for densities taken from 3D simulation of the natural jet in co-flow (a); the forced jet in co-flow with various frequencies: (b) is for frequency $\pi/6$, (c) is for frequency $\pi/9$ and (d) is for frequency $\pi/12$

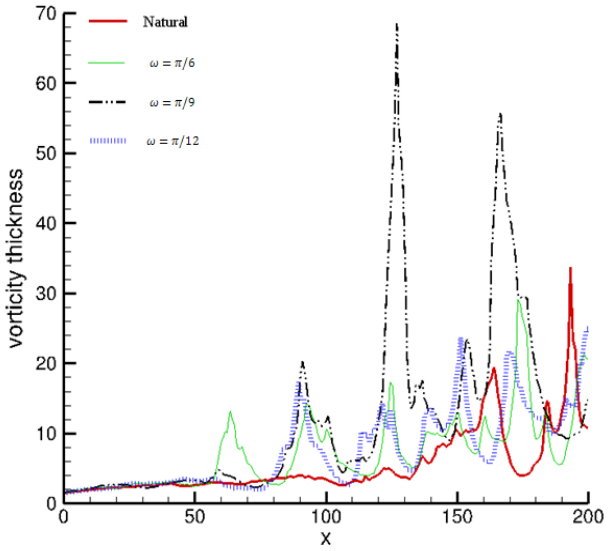

Fig. 3.7. Vorticity thickness for natural jet case and forced jet case with various frequencies

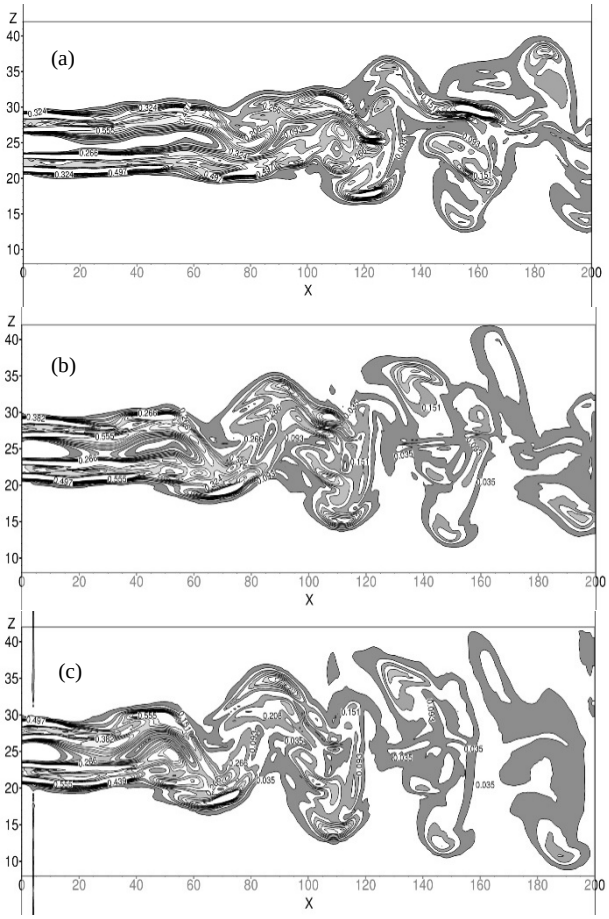

Fig. 3.8. Isolines of vorticity for forced jet in co-flow with frequency $\pi/9$ for various amplitudes: (a) A and B are 0.03, (b) A and B are 0.06 and (c) A and B are 0.1.

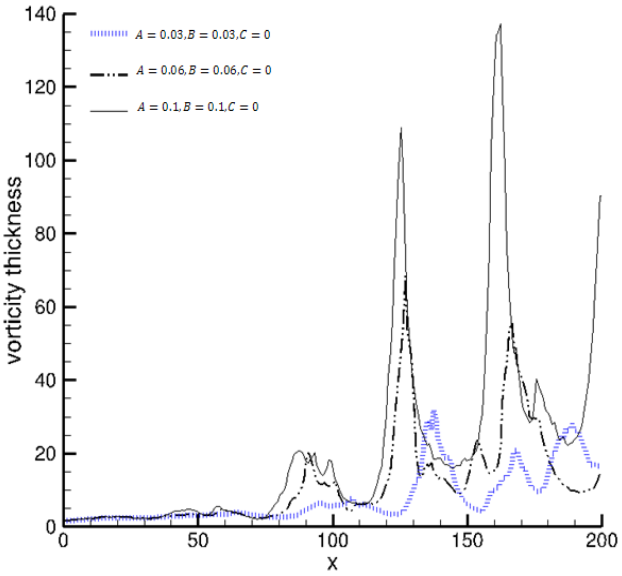

Fig. 3.9. Vorticity thickness δ_ω for the forced jet case with frequency $\pi/9$ and for the various amplitudes.

References:

[1] M.R. Davis, "Measurements in a subsonic turbulent jet using a quantitative schlieren technique", *J. Fluid Mech.*, vol. 46, part 4, pp. 631-656, 1971.

[2] M.R. Davis, "Quantitative schlieren measurements in a supersonic turbulent jet", *J. Fluid Mech.*, vol. 51, part 3, pp. 435-447, 1972.

[3] R.A. Antonia and R.W. Bilger, "An experimental investigation of an axisymmetric jet in a co-flowing stream", *J. Fluid Mech.*, vol. 61, part 4, pp. 805-822, 1973.

[4] J.-L. Borean, D. Huilier and H. Burnage, "On the effect of a co-flowing stream on the structure of an axisymmetric turbulent jet", *Experimental Thermal and Fluid Science*, No. 7, pp. 10-17, 1998.

[5] L.P. Xia and K.M. Lam, "Velocity and concentration measurements in initial region of submerged round jets in stagnant environment and in coflow", *Journal of Hydro-environment Research*, No. 3, pp. 21-34, 2009.

[6] J.J. Charonko and K. Prestridge, "Variable-density mixing in turbulentjets with coflow", *J. Fluid Mech.*, vol. 825, pp. 887-921, 2017.

[7] F. De Gregorio and F. Albano, "Free Compressible Jet Nozzle Investigation", *16th Int. Symp. on Applications of Laser Techniques to Fluid Mechanics*, Lisbon, Portugal, 09-12 July, 2012.

[8] A. J. Saddington, N. J. Lawson and K. Knowles, "Numerical predictions and experiments on supersonic jet mixing from castellated nozzles", *ICAS Congress*, 2002.

[9] M. Maidi and M. Lesieur, "Large eddy simulations of spatially growing subsonic and supersonic turbulent round jets", *Journal of Turbulence*, 6, No.38, 2005

[10] C. Bogey and C. Bailly, "Large eddy simulations of transitional round jets: Influence of the Reynolds number on flow development and energy dissipation", *Physics of Fluids*, No. 18, 065101, 2006.

[11] A. Ghasemi, A. Pereira and X. Li, "Large Eddy Simulation of Compressible Subsonic Turbulent Jet Starting From a Smooth Contraction Nozzle", *Flow Turbulence Combust*, No. 98, pp.83–108,2017.

[12] G. Balarac, M. Lesieur and O. Metais, "Control of coaxial jets by an azimuthal excitation: vortex dynamic and mixing properties", *TSFP digital library*, Vol. 5, 2007.

[13] C.-W. Kuo, J. Cluts and M. Samimy, "Effects of excitation around jet preferred mode Strouhal number in high-speed jets", *Exp. Fluids*, pp. 58-35, 2017.

[14] C. B. da Silva and O. Metais, "Vortex control of bifurcating jets: A numerical study", *Physics of fluids*, Vol. 14, No. 11, pp. 3798-3816, 2002.

[15] K. BMQ Zaman and G. Raman, "Edward J Rice and flow control studies for jets and shear layers at NASA Glenn Research Center", *International Journal of Aeroacustics* 0 (0), pp. 1-15, 2016.

[16] A. Tyliszczak and L. Kuban, "Modelling of liquid sprays in excited jet using large eddy simulation", *TSFP digital library*,Vol. 5, 2007.

[17] M. A. Kamran and J.J. McGurik, "Unsteady predictions of mixing enhancement with steady and pulsed control jets", *AIAA Journal*, Vol. 53, No. 5, pp. 1262 – 1276, 2015.

[18] N. Jarrin, "Synthetic inflow boundary conditions for the numerical simulation of turbulence", Manchester, pp. 247-258, 2008.

[19] M.M. Rogers and R.D. Moser, "The three dimensional evolution of a plane mixing layer: the Kelvin-Helmholtz roll-up", *Journal of Fluid Mechanics*, Vol.243., pp. 183–226, 1992.

[20] J. Kim, P. Moin and R. Moser, "Turbulence statistics in fully developed channel flow at low

Reynolds number", *Journal of Fluid Mechanics*,Vol. 177, pp. 133–166, 1987.

[21] A. Smirnov, S. Shi and I. Celik, "Random flow generation technique for large eddy simulations and particle-dynamics modeling", *Morgantown*, WV26506-6106.

[22] D.Yu. Adamyan, M.H. Strelets and A.K. Travin, "An efficient method of generation of synthetic turbulence at the entrance boundaries of the LES region within the framework of combined RANS-LES approaches to the calculation of turbulent flows", *Mathematical Modeling*,Vol. 23, No. 7, pp. 3-19, 2011.

[23] S. S. Stanley and S. Sarkar, "Simulations of spatially developing two-dimensional shear layers and jets", *Theoretical Computational Fluid Dynamics*, Vol. 9, pp. 121-147, 1997.

[24] Dale A. Hudson, "Numerical simulation of a confined supersonic shear layer", PhD Thesis, pp. 1-181, 1996.

[25] N.D. Sandham and W.C. Reynolds, "Compressible Mixing Layer: Theory and Direct Simulation", *AIAA Journal*, Vol.28, №4, pp.618-623,1989.

[26] T.J. Poinsot, S.K. Lele, "Boundary Conditions for Direct Simulation of Compressible Viscous Flows", *Journal of Computational Physics*, № 101, pp.104-129, 1992.

[27] A.Beketaeva, A. Naimanova, "Flow structure of the transverse jet interaction with supersonic flow for moderate to high pressure ratios", *International journal of mechanics*, Vol.12, pp. 88-95, 2018.

[28] A. Beketaeva, P.Bruel and A. Naimanova, "Vortical structures behind a transverse jet in a super-sonic flow at high jet to crossflow pressure ratios", *J. Appl. Mech. and Tech.Phys*.,Vol. 56, No 5, pp. 777-788– 2015.

[29] M. Samimy and G.S.Elliott. "Effects of compressibility on the characteristics of free shear layers", *AIAA Journal*, Vol. 28, No. 3, pp. 439-445,1990